symmetry

MDPI

Article

A Wideband and Ultra-Thin Metamaterial Absorber Based on Resistive FSS

Zhongliang Lv, Zelun Li *, Yu Han, Yujiang Cao and Lin Yang

College of Mechanical and Power Engineering, Chongqing University of Science and Technology, Chongqing 401331, China; 2010024@cqust.edu.cn (Z.L.); 2020203039@cqust.edu.cn (Y.H.); 2021203230@cqust.edu.cn (Y.C.); 2020203030@cqust.edu.cn (L.Y.)

* Correspondence: zelunli@cqust.edu.cn; Tel.: +86-186-2302-8421

Abstract: A wideband, ultra-thin, wide-angle and polarization-insensitive metamaterial absorber with a single-layer resistive frequency selective surface (FSS) is proposed. The simulated results show that the absorption rate of the absorber is greater than 90% in a frequency range of 24.1–42.6 GHz, and the relative absorption bandwidth is up to 55.47%. The thickness of the structure is 1.2 mm, which is 0.088 λ and 0.156 λ for the lowest and highest frequencies, respectively. The power loss density is analyzed to explore the mechanism of the absorption and the resistive film layer is important for the wideband absorption. Meanwhile, a strong absorption for oblique incidence with wide angle and the characteristics of polarization insensitivity are achieved for the proposed design.

Keywords: metamaterial absorber; wideband absorption; resistance film

Citation: Lv, Z.; Li, Z.; Han, Y.; Cao, Y.; Yang, L. A Wideband and Ultra-Thin Metamaterial Absorber Based on Resistive FSS. *Symmetry* **2022**, *14*, 1148. https://doi.org/10.3390/sym14061148

Received: 1 April 2022
Accepted: 28 May 2022
Published: 2 June 2022

1. Introduction

Metamaterials are artificial structures which have extraordinary physical properties. Due to unique benefits, the metamaterials have attracted intense attention [1–3]. Recently, with the development of metamaterial research, researchers have made many great achievements in the fields of negative refraction materials [4,5], invisible cloaking [6,7], the miniaturization of antennas and microwave devices [8,9].

The concept of the metamaterial absorber (MA) was presented by Landy et al. [10]. The advantages of the metamaterials, such as size minimization and small thickness, have attract researchers. However, this type of absorbing structure has quite narrow bandwidth [11–13]. Recently, MA with multi-layer [14,15], multi-resonator [16] and lumped element structures [17–19] have been proposed for wideband absorption, these designs suffer from large thickness and size. Moreover, the fabrication of such structures is quite difficult and thus impedes their application in practice.

These limitations have been overcome by compact, ultra-thin MA designs based on resistive film. In recent years, it was found that the absorption band can be enlarged by increasing the resistance of the resonant structure [20]. Based on this theory, the resistive frequency selective surface (FSS) has been widely investigated [21–27]. In this paper, an ultrathin, polarization-insensitive and wide-angle MA based on a single-layer resistive FSS has been presented. The simulated reflection and absorption show that the absorption of the MA is greater than 90% in a frequency range of 24.1–42.6 GHz, and the absorption bandwidth is 18.5 GHz. Meanwhile, the thickness of the proposed structure is 1.2 mm, which is 0.088 λ and 0.156 λ for the lowest and highest frequencies, respectively. Compared with other designs, our proposed structure exhibits wider absorption bandwidth and smaller absorber thickness. We explored the mechanism of the absorber and the influences of various dimensional parameters on absorption spectrum. Moreover, a strong absorption for oblique incidences with wide angle and the characteristics of polarization insensitivity are both achieved theoretically. The advantages of the proposed structure,

such as thin thickness and compact size, provide an effective way to design broadband metamaterial absorbers.

2. Design of the Absorber

The cell of the absorber is shown in Figure 1. The proposed MA structure has four components: a single-layer resistive FSS in the form of a ring loop as an impedance sheet, a packed layer, a dielectric substrate and a copper plate as a perfect electric conductor. The optimal geometrical parameters of the MA are as follows: a = 8.5 mm, l = 3.9 mm, w = 2.3 mm, t = 0.017 mm, d = 0.1 mm, and h = 1.1 mm. The ring-shaped resistive FSS is made of the material with permittivity ε of 3.4 and conductivity σ of 100 S/m. The dielectric material with the permittivity ε of 3.5 is served as the substrate and the packed layer. A lossy copper plate with a conductivity of σ = 5.8 × 10^7 S/m is used as the ground plane.

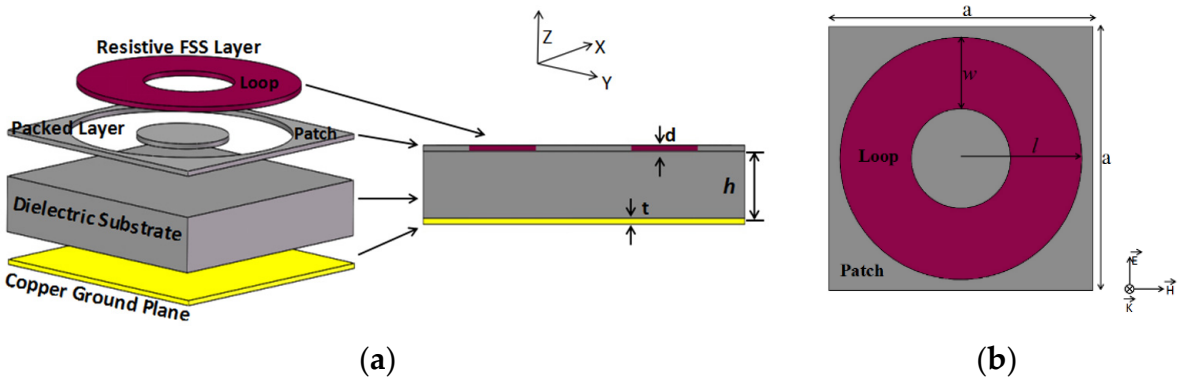

Figure 1. (**a**) Cell of the absorber. (**b**) Layout of the resonant structure.

The simulations were carried out with CST Microwave Studio by using the finite-element frequency-domain method. The unit cell boundaries are utilized in the x and y axis, and the Floquet port condition is applied in the z axis. A plane wave with E field polarized along the x-axis is incident to the MA along the z-axis.

The absorptivity is calculated as: $A = 1-|S_{11}|_2-|S_{21}|^2$, where S_{11} is the reflection and S_{21} is the transmission coefficient, respectively. S_{21} is zero due to the copper ground, thus the absorptivity can be calculated as: $A = 1-|S_{11}|^2$.

The simulated absorption spectrum of the proposed structure is shown in Figure 2. It is observed that there are two resonance frequencies of 28.93 and 38.00 GHz with absorptivity of 94.1% and 98.0%, respectively. Meanwhile, the absorption of the proposed absorber is more than 90% from 24.1 to 42.6 GHz, with a bandwidth of 18.5 GHz. The relative bandwidth can be defined by $W_{RAB} = 2(f_U - f_L)/(f_U + f_L)$, where f_U and f_L are the upper and lower frequencies with the absorption greater than 90%. From the calculations, the relative bandwidth for the proposed MA is 55.47%.

The proposed absorber has been compared with recently reported MAs in Table 1. Compared with other single-layer designs, the proposed absorber exhibits wider absorption bandwidth and smaller structure thickness. Meanwhile, the simple pattern shape of the proposed structure makes it more feasible for fabrication. It should be noted that, although the multi-layer FSS design can further increase the absorption bandwidth, the fabrication of such a structure would face more challenges, as both the preparation and alignment error between the adjacent FSS layers would decrease the absorption performance significantly.

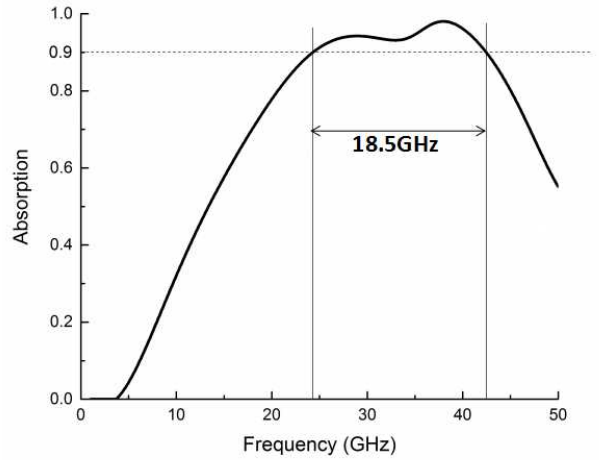

Figure 2. Absorption spectrum of the proposed MA under normal incidence.

Table 1. Recently reported broadband MAs with resistive FSS.

Absorber	Unit Cell Size (mm)	Thickness (mm)	Bandwidth (GHz)	Absorptivity	Layers
[22]	8 × 8	2.1	18.3 (10.7–29)	>90%	one
[23]	20 × 20	0.75	34.5 (7.5–42)	>90%	two
[24]	3.75 × 3.75	6.0	52.8 (6.8–59.6)	>90%	four
[25]	4.6 × 4.6	1.44	<8 (In the range of 20–30)	>90%	one
[26]	20 × 20	3.3	9.8 (6.58–16.38)	>90%	one
This paper	8.5 × 8.5	1.2	18.5 (24.1–42.6)	>90%	one

3. Discussion of Absorption Mechanism

The cell of the proposed structure consists of ring-shaped resistive FSS (the loop), and the packed dielectric materials (the patch). To illustrate the absorption mechanism of this absorber, the absorptivity with different combinations is shown in Figure 3. As shown in Figure 3, by replacing the resistive FSS with metal loop, the wideband absorption could not be achieved. Hence, the resistive FSS is important for electromagnetic wave absorption. Moreover, if there is no dielectric patch, one can enable a wider absorption band at upper frequencies. However, the resistive FSSs could not be well supported without the patches, as we keep them in this design.

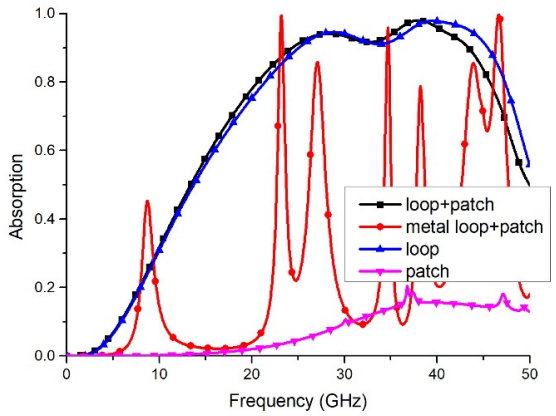

Figure 3. Absorptivity for different combinations of structures.

The normalized input impedances $Z(f)$ at the free space can be expressed as [27]:

$$Z(f) = \sqrt{\frac{(1+S_{11})^2 - S_{21}^2}{(1-S_{11})^2 - S_{21}^2}}$$

Figure 4 shows the calculated normalized input impedance. It is seen that the relative impedances at two peak resonance frequencies are 1.038 + 0.183i and 1.018 + 0.055i, respectively. Moreover, for frequency ranging from 24.1 to 42.6 GHz, the real parts are close to unity and imaginary parts are close to zero. Hence, the normalized input impedances of the MA approximately match the free-space impedance in such a bandwidth, leading to a high absorption of incident wave.

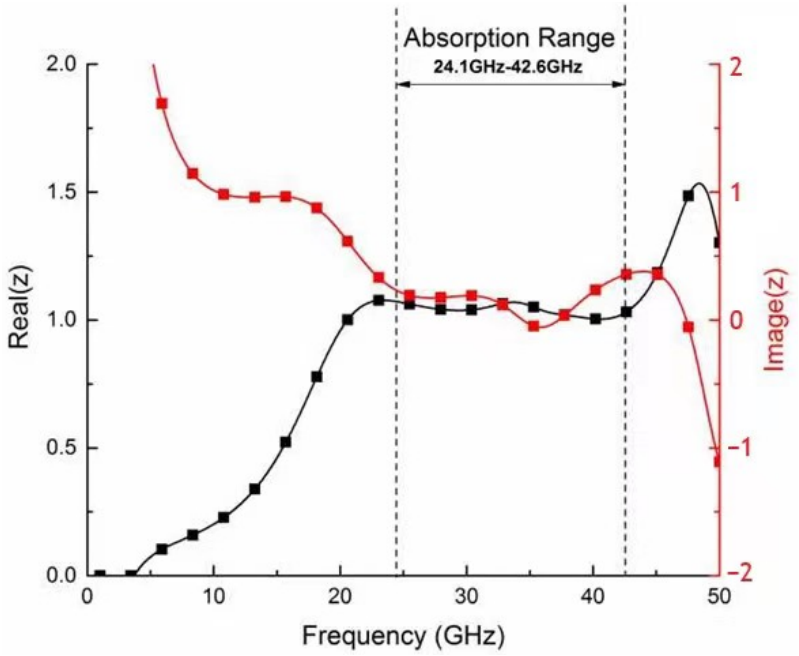

Figure 4. Calculated input impedance of the proposed MA.

In order to explore the absorption mechanism, we calculated the electric field distributions for two peak absorption frequencies. As shown in Figure 5a, the first resonant mode for 28.93 GHz is originated from the strong coupling between the FSS rings. However, the electric field is concentrated on the patch for the second resonant mode at 38.00 GHz (Figure 5b). We further calculated the absorption of the ring-shaped resistive FSS with different conductivities and the dielectric substrate with different loss tangents, and the results are shown in Figure 6. With the increase in the conductivity of the resistance film, as shown in Figure 6a, the absorptivity of the proposed structure decreases. Higher conductivity of the FSS leads to a smaller ohmic loss, as a result, the incident wave absorption decreases. However, it is observed from Figure 6b that the absorptivity for different loss conditions of the dielectric substrate is almost the same. Hence, the dielectric loss in the substrate contributes little on the total power consumption. The calculated surface loss at the resistive FSS and the power loss distribution on the dielectric substrate for two peak absorptions presented in Figure 7 confirm the phenomenon, where the resistive film layer contributes 99.54% and 99.67% of power absorption for the first and second resonant mode, respectively.

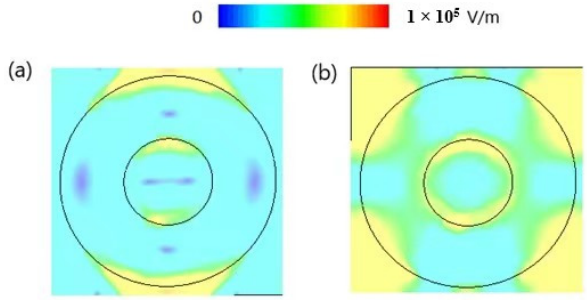

Figure 5. Calculated electric field distributions for two peak absorption frequencies of (**a**) 28.93 GHz and (**b**) 38.00 GHz.

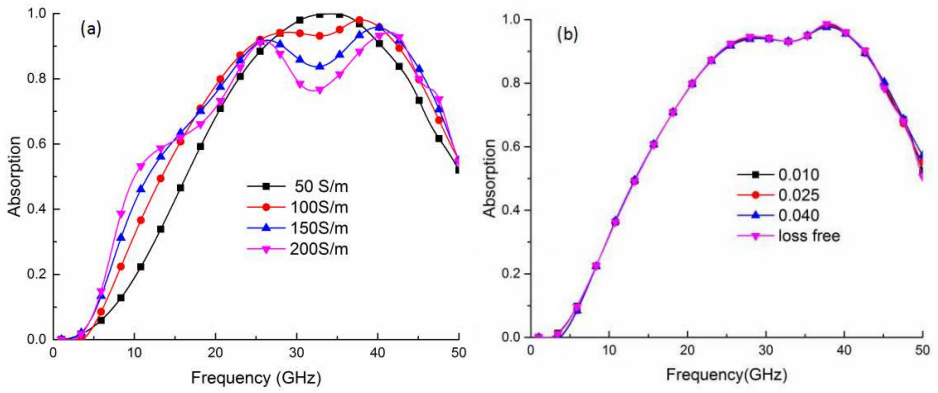

Figure 6. Absorption spectra of the proposed MA (**a**) for different FSS conductivities and (**b**) for different substrate loss conditions.

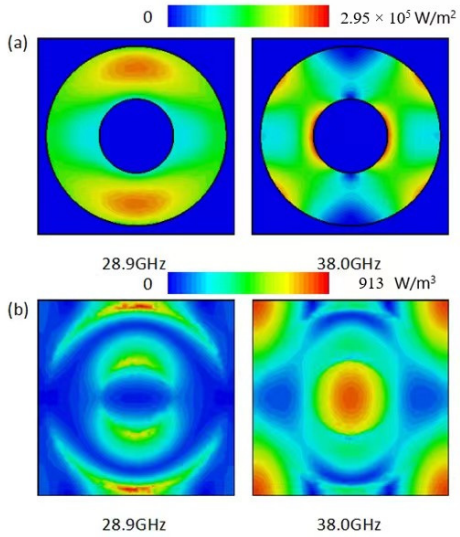

Figure 7. (**a**) Distribution of the surface losses on the ring-shaped resistive FSS. (**b**) Distribution of the power loss on the dielectric substrate.

4. Parametric Studies of Absorption Spectrum

To better explore the influence of the structural dimensions, we simulated the absorption spectra with different structural dimensions. For example, the influence of the resistive FSS' outer radius (l), the width of loop (w), as well as the height of the dielectric layer (h), are investigated, the simulation results are presented in Figure 8.

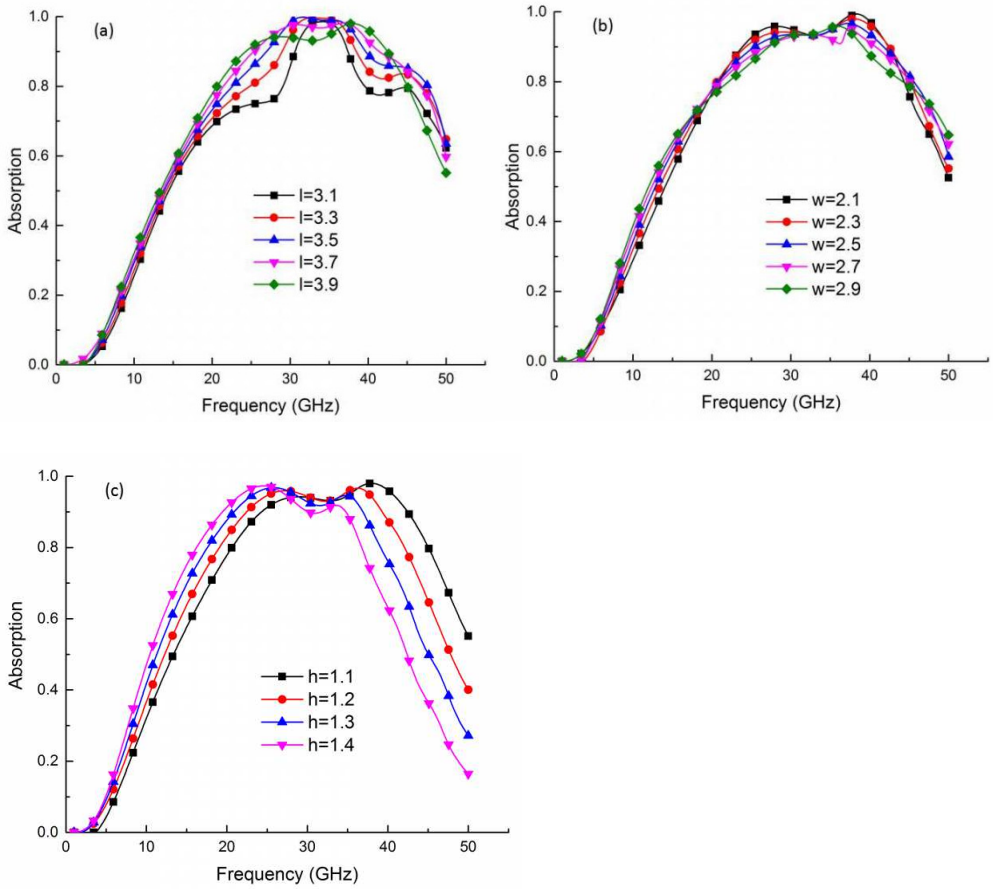

Figure 8. Simulated absorption spectra for different structural parameters: (**a**) resistive FSS' outer radius, l, (**b**) width of loop, w, and (**c**) height of the dielectric layer, h.

As shown in Figure 8a, with the increase in outer radius l, the absorption bandwidth becomes wider. For example, with l equaling 3.1 mm, the bandwidth is only 6.76 GHz (30.65 to 37.41 GHz) with more than 90% absorptivity. However, when l increases to 3.9 mm, the bandwidth with 90% absorptivity covers the frequency range from 24.1 to 42.6 GHz. As mentioned above, the first resonance frequency is sensitive to the outer ring radius l. By increasing the l, the first resonance frequency shows a blueshift, which enlarged the absorption bandwidth. As shown in Figure 8b, by varying the loop width w from 2.1 mm to 2.9 mm, the two resonant frequencies did not show a clear change. This is due to the fact that, when the outer ring radius l is fixed, the change in the loop width w has little effect on both the resonant modes; hence, the absorption is insensitive to it. Moreover, it is observed in Figure 8c that, as the substrate thickness h increases from 1.1 mm to 1.4 mm, both the resonance frequencies redshifted. With the decrease of h, the equivalent capacitance of the resonator increases, and the resonance frequencies shift towards lower frequencies.

5. Influence of Polarization and Oblique Incidence

The proposed MA is analyzed for different polarization angles. As shown in Figure 9, the absorption spectrum is constant for different polarizations. Due to the symmetry of the designed structure, it maintains a stable property of electromagnetic absorption. Therefore, the proposed absorber exhibits polarization insensitivity.

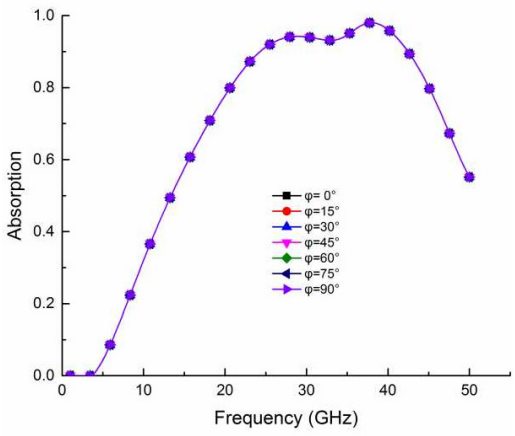

Figure 9. Absorption for different polarization angles.

The influence of the incidence angles θ on the absorption is simulated and shown in Figure 10. For TE polarization, as illustrated in Figure 10a, the absorption is constant for incident angles up to 15°. With the continuous increase in incident angle θ, the absorption bandwidth decreases. However, even with the incident angle reaching 60°, the absorber exhibits wideband absorption from 29.42 to 46.52 GHz with an absorptivity of greater than 70%. Meanwhile, as shown in Figure 10b, the MA maintains wideband absorption for TM polarization with wide angles. For example, the absorption bandwidth increases to 24.05 GHz (23.79–47.84 GHz) when the incident angle reaches 60°. Hence, the proposed structure has good broadband absorption for oblique incidence with wide angles.

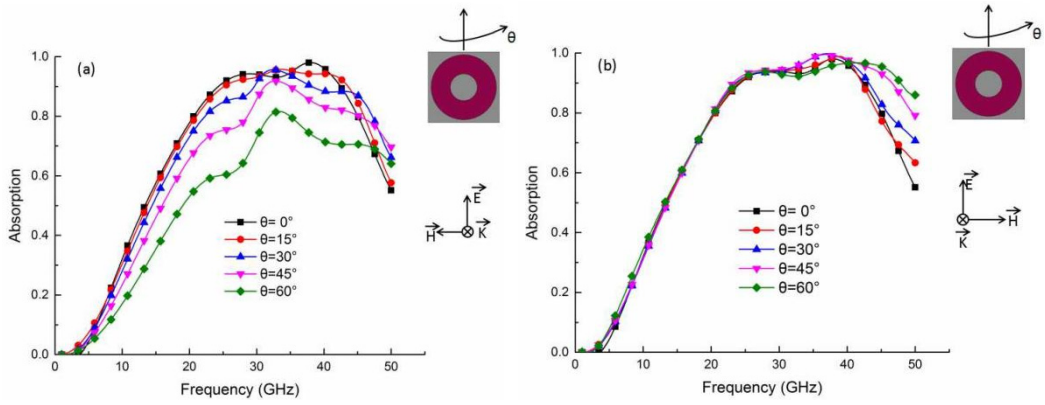

Figure 10. (**a**) Simulated absorption with different oblique incident angles θ for (**a**) TE and (**b**) TM polarizations.

6. Conclusions

This paper presents the design and analysis of a simple wideband MA based on the single-layer resistive FSS. The structure provides wideband absorption (24.1–42.6 GHz) with absorption rate above 90%, and the relative absorption bandwidth is 55.47%. The structure only has a thickness of 1.2 mm, which is 0.088 λ and 0.156 λ for the lowest and highest frequencies. The field and power loss distributions are investigated to show the absorption mechanism of the proposed absorber, while the simulated results show that the resistive FSS is important for electromagnetic wave absorption. The effects of geometrical parameters on absorption bandwidth are explored to optimize the MA design. The absorption bandwidth can be enlarged by increasing the outer radius of the FSS ring. Meanwhile, the resonance frequencies shift towards lower frequencies with the increase in substrate thickness. Moreover, the characteristics of polarization insensitivity are achieved theoretically. The absorption dependence on incidence angle was further investigated. For TE polarization, the absorber exhibits wideband absorption from 29.42 to

46.52 GHz at the incident angle of 60° with an absorptivity of greater than 70%. For TM polarization, the absorption bandwidth with absorptivity above 90% increases to 24.05 GHz (23.79–47.84 GHz) when the incident angle reaches up to 60°. Hence, the proposed MA exhibits good broadband absorption performance with a wide range of incident angles. The compact and simple design has potential application in constructing wideband absorbers.

Author Contributions: Writing—original draft, Z.L. (Zelun Li); Writing—review & editing, Z.L. (Zhongliang Lv); software, Y.H.; formal analysis, Y.C.; validation, L.Y. All authors have read and agreed to the published version of the manuscript.

Funding: This research was supported by the National Natural Science Foundation of China (No. 51705053), Chongqing Research Program of Basic Research and Frontier Technology (No. cstc2018jcyjAX0291, cstc2019jcyj-msxmX0720), and the Science and Technology Research Program of Chongqing Municipal Education Commission (No. KJQN201801536, KJZD-K201901503).

Institutional Review Board Statement: Not applicable.

Informed Consent Statement: Not applicable.

Data Availability Statement: Not applicable.

Acknowledgments: The authors wish to sincerely thank to the anonymous reviewers for their constructive comments.

Conflicts of Interest: The authors declare no conflict of interest.

References

1. Smith, D.R.; Pendry, J.B.; Wiltshire, M.C.K. Metamaterials and negative refractive index. *Science* **2004**, *305*, 788–792. [CrossRef]
2. Ferrari, L.; Wu, C.; Lepage, D.; Zhang, X.; Liu, Z. Hyperbolic metamaterials and their applications. *Prog. Quant. Electron.* **2015**, *40*, 1–40. [CrossRef]
3. Liu, R.P.; Zhao, Z.Y.; Ji, C.L. Metamaterials beyond negative refractive index: Applications in telecommunication and sensing. *Sci. China Technol. Sci.* **2016**, *59*, 1007–1011. [CrossRef]
4. Wang, S.; Garet, F.; Blary, K.; Lheurette, E.; Coutaz, J.L.; Lippens, D. Experimental verificatio of negative refraction for a wedge-type negative index metamaterial operating at terahertz. *Appl. Phys. Lett.* **2010**, *97*, 11555.
5. Valentine, J.; Zhang, S.; Zentgraf, T.; Ulin-Avila, E.; Genov, D.A.; Bartal, G.; Zhang, X. Three-dimensional optical metamaterial with a negative refractive index. *Nature* **2008**, *455*, 376–379. [CrossRef]
6. Chen, H.; Wu, B.I.; Zhang, B. Electromagnetic wave interactions with a metamaterial cloak. *Phys. Rev. Lett.* **2007**, *99*, 063903. [CrossRef]
7. Ni, X.; Wong, Z.; Mrejen, M.; Wang, Y.; Zhang, X. An ultrathin invisibility skin cloak for visible light. *Science* **2015**, *349*, 1310–1314. [CrossRef]
8. Kang, M.; Feng, T.; Wang, H.; Li, J. Wave front engineering from an array of thin aperture antennas. *Opt. Express* **2012**, *20*, 15882–15890. [CrossRef]
9. Deng, G.; Lv, K.; Sun, H.; Yang, J.; Yin, Z.; Chi, B.; Li, X. An ultra-broadband and optically transparent metamaterial absorber based on multilayer indium-tin-oxide structure. *J. Phys. D Appl. Phys.* **2021**, *54*, 165301. [CrossRef]
10. Landy, N.I.; Sajuyigbe, S.; Mock, J.J. Perfect metamaterial absorber. *Phys. Rev. Lett.* **2008**, *100*, 207402. [CrossRef]
11. Ayop, O.; Rahim, M.K.A.; Murad, N.A. Dual-resonant polarization-independent and wide-angle metamaterial absorber in X-band frequency. *Appl. Phys. A-Mattr.* **2016**, *122*, 374. [CrossRef]
12. Bhattacharyya, S.; Vaibhav Srivastava, K. Triple band polarization-independent ultra-thin metamaterial absorber using electric field-driven LC resonator. *J. Appl. Phys.* **2014**, *115*, 93–102. [CrossRef]
13. Shen, X.; Cui, T.J.; Zhao, J. Polarization-independent wide-angle triple-band metamaterial absorber. *Opt. Express* **2011**, *19*, 9401–9407. [CrossRef] [PubMed]
14. Sun, J.; Liu, L.; Dong, G. An extremely broad band metamaterial absorber based on destructive interference. *Opt. Express* **2011**, *19*, 21155–21162. [CrossRef] [PubMed]
15. Xiong, H.; Hong, J.S.; Luo, C.M. An ultrathin and broadband metamaterial absorber using multi-layer structures. *J. Appl. Phys.* **2013**, *114*, 064109. [CrossRef]
16. Deng, G.; Chen, W.; Yu, Z.; Cai, F.; Yang, J.; Yin, Z. 3D-printed dielectric resonator-based ultra-broadband microwave absorber using water substrate. *J. Electron. Mater.* **2022**, *51*, 2221–2227. [CrossRef]
17. Ramya, S.; Srinivasa Rao, I. A compact ultra-thin ultra-wideband microwave metamaterial absorber. *Microw. Opt. Technol. Lett.* **2017**, *59*, 1837–1845. [CrossRef]
18. Sood, D.; Tripathi, C.C. A Compact Ultrathin Ultra-wideband Metamaterial Microwave Absorber. *J. Microw. Optoelectron. Electromagn. Appl.* **2017**, *16*, 514–528. [CrossRef]

19. Lee, J.; Lim, S. Bandwidth-enhanced and polarisation-insensitive metamaterial absorber using double resonance. *Electron. Lett.* **2011**, *47*, 8–9. [CrossRef]
20. Zhang, H.B.; Zhou, P.H.; Lu, H.P. Resistance selection of high impedance surface absorbers for perfect and broadband absorption. *IEEE Tran. Antennas Propag.* **2013**, *61*, 976–979. [CrossRef]
21. Lu, Y.; Chi, B.; Liu, D.; Gao, S.; Gao, P.; Huang, Y.; Yang, J.; Yin, Z.; Deng, G. Wideband Metamaterial Absorbers Based on Conductive Plastic with Additive Manufacturing Technology. *ACS Omega* **2018**, *3*, 11144–11150. [CrossRef]
22. Li, M.; Xiao, S.Q.; Bai, Y.Y. An ultrathin and broadband radar absorber using resistive FSS. *IEEE Antennas Wirel. Propag. Lett.* **2012**, *11*, 748–751.
23. Cheng, Y.Z.; Nie, Y.; Gong, R.Z. Design of an ultrathin and wideband metamaterial absorber based on resistance film and fractal frequency selective surface. *Acta Phys. Sin.* **2013**, *62*, 044103. [CrossRef]
24. Lin, B.Q.; Wei, W.; Da, X.Y.; Du, S.S.; Li, W. A Novel ultra-Broadband Metamaterial Absorber Based on Multilayer Resistance Films. *Acta Pharmacol. Sin.* **2014**, *42*, 607–610.
25. Yang, S.; Chen, Y.; Wang, W.; Kang, J.; He, X. A metamaterial based urltrawideband absorber with polarizagion independent. *Chin. J. Radiol.* **2015**, *30*, 834–837.
26. Deng, G.; Lv, K.; Sun, H.; Hong, Y.; Zhang, X.; Yin, Z.; Yang, J. Wideband absorber based on conductive ink frequency selective surface with polarization insensitivity and wide-incident-angle stability. *Nanomater. Nanotechnol.* **2020**, *10*, 1847980420935718. [CrossRef]
27. Smith, D.R.; Vier, D.C.; Koschny, T. Electromagnetic parameter retrieval from inhomogeneous metamaterials. *Phys. Rev. E* **2005**, *71*, 036617. [CrossRef]